Spontaneous loop supercurrents from interference-selected Josephson-island winding states

Henry Sheehy[1, 2]

[1] *School of Physical Sciences, University of Kent, Canterbury CT2 7NH, United Kingdom*
[2] *QuantaLumin*

(Dated: June 16, 2026)

We study spontaneous loop-supercurrent selection in reduced superconducting circuits with attractive superconducting regions coupled through repulsive normal channels. The mechanism is interference selection: a phase texture can lower the energy when destructive interference suppresses anomalous density on a costly normal region. Compact C3 molecules provide the clean analytic rule, because the $m = \pm 1$ winding textures satisfy $1 + \omega + \omega^2 = 0$ and therefore node an active central repulsive site. Compact C4 molecules and clusters expose the obstruction: staggered order also nodes the centre and naturally cancels nearest-neighbour normal paths, so a square loop requires separated diagonal or outer channels to make winding uniquely favourable. Unrestricted microscopic molecules, clusters, tubes, and screw-cell crystals preserve the winding texture but remain too stiff or too amplitude-starved to make it the robust ground state. We then separate condensate formation from phase selection in a Josephson-island model. For a long, soft outer-channel device we find a strict self-consistent Hartree–Fock–Gor'kov winding minimum with degenerate time-reversed partners, $F_{\rm wind} - F_{\rm nonwind} \simeq -2.386 \times 10^{-3}$, and a maximum residual below 5×10^{-5}. The result is an existence proof for a time-reversal-symmetric Hamiltonian selecting a time-reversal-breaking loop-current state without imposed flux or Peierls phases.

I. INTRODUCTION

Josephson circuits are a natural setting for phase frustration and current-carrying superconducting states [1, 2]. The question addressed here is sharper than whether a current can be imposed by external flux. We ask whether a time-reversal-symmetric superconducting device can choose a pair of degenerate, time-reversed winding states as its self-consistent ground state. Such a state would be a finite-device analogue of spontaneous time-reversal symmetry breaking familiar from unconventional superconductivity [3–5], but selected by real-space interference rather than by explicitly building a chiral order parameter into the Hamiltonian.

The central difficulty is that winding costs phase stiffness. A loop phase texture must twist around the device, and in a compact microscopic molecule that cost is large. The compensating energy scale is the repulsive-channel Gor'kov penalty: if a normal region has positive interaction or repulsive anomalous-density cost, a superconducting texture can gain energy by placing a node on that region. This produces a concrete design problem. The normal channel must be occupied in nonwinding branches, suppressed in the winding branch, and long or soft enough that the saved interaction energy exceeds the stiffness cost.

Figure 1 summarizes the resulting logic. C3 gives the clean node rule. C4 introduces the staggered competitor. Screw-separated channels restore a winding-specific penalty. Long, soft Josephson-island channels then provide a finite self-consistent realization.

II. MODEL AND SELF-CONSISTENCY

We consider finite tight-binding superconducting devices with an attractive region A and repulsive or normal regions N. A minimal microscopic form is

$$H = \sum_{ij,\sigma} h_{ij}^{(0)} c_{i\sigma}^\dagger c_{j\sigma} + \sum_i U_i n_{i\uparrow} n_{i\downarrow}, \tag{1}$$

with $U_i < 0$ on superconducting islands and $U_i > 0$ or no attractive instability on normal sites. For the island calculations below the same local interaction profile is written in region language: $U_i = -U$ on superconducting islands, $U_i = +V$ on inner normal channels, and $U_i = +W$ on outer normal channels. All hoppings and interaction constants are real, so the Hamiltonian is time-reversal symmetric; no flux or Peierls phase is imposed.

The HFG fields are obtained from the normal and anomalous contractions

$$\rho_{i\sigma,j\sigma'} = \langle c_{j\sigma'}^\dagger c_{i\sigma} \rangle, \qquad \kappa_i = \langle c_{i\downarrow} c_{i\uparrow} \rangle. \tag{2}$$

For the onsite interaction, Wick factorization gives

$$\begin{aligned} n_{i\uparrow} n_{i\downarrow} \simeq\ & \langle n_{i\uparrow} \rangle n_{i\downarrow} + n_{i\uparrow} \langle n_{i\downarrow} \rangle - \langle n_{i\uparrow} \rangle \langle n_{i\downarrow} \rangle \\ & + \kappa_i c_{i\uparrow}^\dagger c_{i\downarrow}^\dagger + \kappa_i^* c_{i\downarrow} c_{i\uparrow} - |\kappa_i|^2. \end{aligned} \tag{3}$$

The spin-flip Fock terms vanish in the accepted nonmagnetic island ansatz. The resulting quadratic HFG Hamiltonian is

$$\begin{aligned} H_{\rm HFG} = & \sum_{ij,\sigma} (h_{ij}^{(0)} + \Sigma_{ij,\sigma}) c_{i\sigma}^\dagger c_{j\sigma} \\ & + \sum_i \left(\Delta_i c_{i\uparrow}^\dagger c_{i\downarrow}^\dagger + \Delta_i^* c_{i\downarrow} c_{i\uparrow} \right) + E_{\rm dc}, \end{aligned} \tag{4}$$

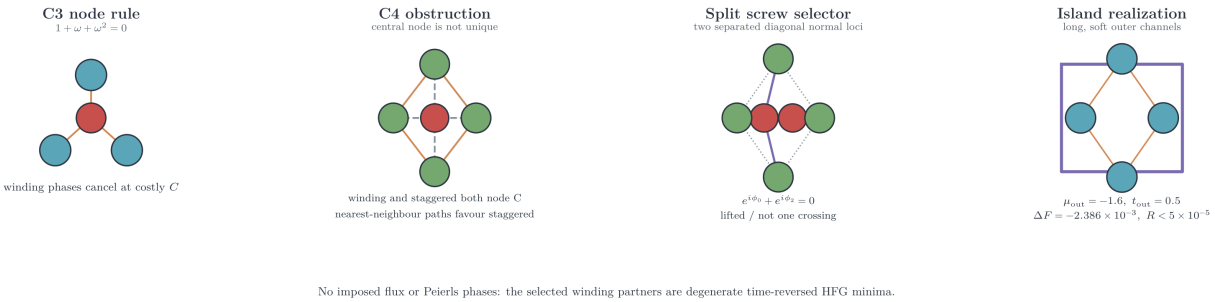

FIG. 1. Mechanism-to-device overview. In C3, the winding phase sum cancels the central repulsive site. In C3 clusters, the same central node is retained, but a loop supercurrent also requires outer hopping around the attractive regions. In C4, winding and staggered textures both node the centre, while staggered also cancels nearest-neighbour normal paths. A split-screw construction uses two separated diagonal normal loci so that winding suppresses same-phase diagonal anomalous density without collapsing to a single planar crossing. The final island device supplies superconducting amplitude and uses long, soft outer channels to reduce winding stiffness. This single schematic collects the microscopic design lessons used below: active antinodes must exist in nonwinding branches, winding must remove them by interference, and the phase twist must be spread over a sufficiently soft path.

with local fields

$$\Sigma_{ii,\uparrow} = U_i\langle n_{i\downarrow}\rangle, \qquad \Sigma_{ii,\downarrow} = U_i\langle n_{i\uparrow}\rangle, \qquad \Delta_i = U_i\kappa_i. \tag{5}$$

The double-counting constant subtracts the inserted contractions,

$$E_{\rm dc} = -\sum_i U_i\left(\langle n_{i\uparrow}\rangle\langle n_{i\downarrow}\rangle - |\kappa_i|^2\right), \tag{6}$$

and is included in every branch free energy. In the folded spin-singlet Nambu basis

$$\Psi = (c_{1\uparrow},\ldots,c_{N\uparrow},c^\dagger_{1\downarrow},\ldots,c^\dagger_{N\downarrow})^T, \tag{7}$$

the BdG matrix is

$$\mathcal{H}_{\rm BdG} = \begin{pmatrix} h^{(0)}+\Sigma_\uparrow-\mu & \Delta \\ \Delta^\dagger & -(h^{(0)}+\Sigma_\downarrow-\mu)^T \end{pmatrix}. \tag{8}$$

Self-consistency means recomputing ρ and κ from the occupied quasiparticle states of Eq. (8), updating Eq. (5), and iterating until the maximum field residual falls below the quoted tolerance. For a generic active field $\Phi_\alpha \in \{\Delta_i,\Sigma_i,\ldots\}$ the damped update is

$$\Phi_\alpha^{(m+1)} = (1-\gamma)\Phi_\alpha^{(m)} + \gamma\Phi_{\alpha,\rm cand}^{(m)}, \tag{9}$$

with residual

$$R^{(m)} = \max_{\alpha\in\mathcal{S}}\left|\Phi_{\alpha,\rm cand}^{(m)} - \Phi_\alpha^{(m)}\right|. \tag{10}$$

Linear mixing is used in difficult cases; the unresolved side points discussed below contract slowly rather than oscillating between two branch solutions.

The branch free energy is evaluated from the BdG spectrum and double-counting terms. At $T=0$ the implementation records the common folded-spin convention

$$F_{\rm HFG} = -\frac{1}{2}\sum_\nu |E_\nu| + \frac{1}{2}\,{\rm Tr}\,H_{ee} + F_{\rm Gorkov} + F_{\rm Hartree} + F_{\rm Fock}, \tag{11}$$

where $H_{ee} = h^{(0)} + \Sigma_\uparrow - \mu$. The Gor'kov, Hartree, and Fock terms are the corresponding double-counting constants, decomposed by island, inner-channel, and outer-channel masks. The trace and folded-spin normalization are common to all branches, so branch ordering is unaffected by the convention. The decomposition is used to distinguish a genuine repulsive-channel saving from a trivial loss of superconducting amplitude [6].

III. INTERFERENCE SELECTION

For a repulsive normal site coupled symmetrically to islands with phases ϕ_j, the induced anomalous amplitude is controlled by a phase sum,

$$\kappa_N \propto \sum_j a_j e^{{\rm i}\phi_j}, \tag{12}$$

where a_j includes hopping and spectral weights. If symmetry or geometry makes this sum vanish, the repulsive Gor'kov cost is suppressed.

This is not enough by itself. The free energy also contains the spectral cost of twisting the superconducting phase, Hartree/Fock relaxation, and competition with nonwinding phase patterns. The branch-selection criterion used throughout this work is therefore direct: all candidate branches are iterated under the same self-consistency standard, and the winner is the converged branch with the lowest HFG free energy. Current and time-dependent diagnostics are used only after the static branch is selected.

Candidate geometries were generated in two stages. First, susceptibility and genetic searches proposed parameter sets where the normal-state anomalous response placed large antinodes on repulsive loci that winding can cancel. The genome included chemical potentials, interaction strengths, island separation, outer-channel width

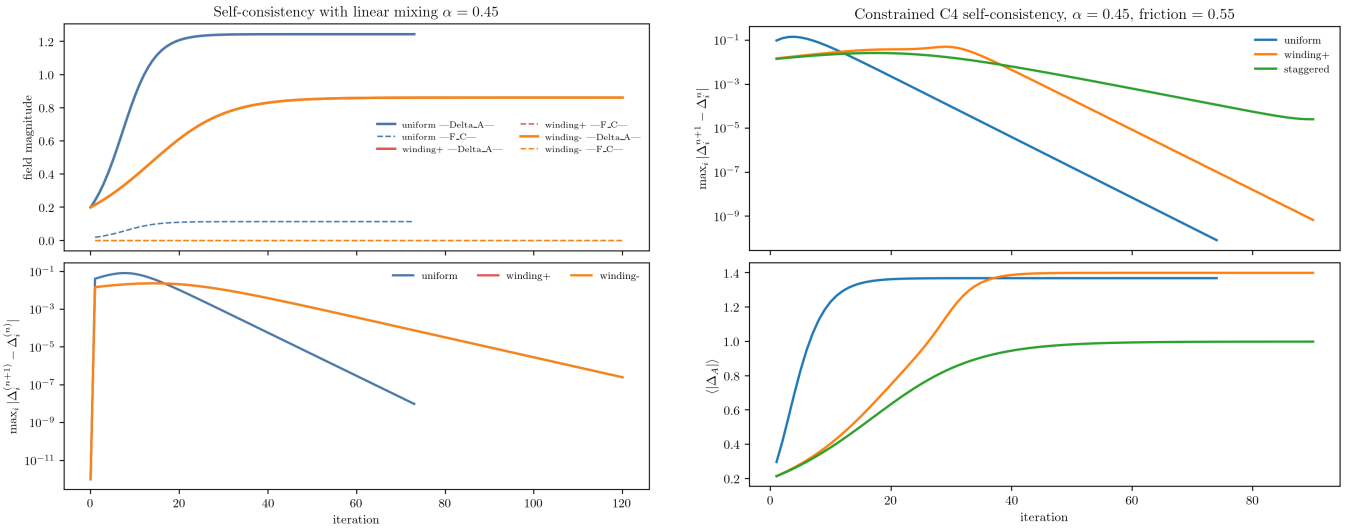

FIG. 2. Representative self-consistent mean-field iteration histories in the compact microscopic problems. Left: the C3 molecule with linear mixing $\alpha = 0.45$ shows the field amplitudes saturating and the maximum update residual decaying over iterations for uniform and winding seeds. Right: the constrained C4 molecule with $\alpha = 0.45$ and friction 0.55 shows uniform, winding, and staggered branches converging at different rates. These examples document that branch labels are followed by actual fixed-point iteration rather than by a one-shot imposed texture; the branch free energy after convergence remains the selection criterion.

and contact geometry, and inner-sheet shape parameters. The fitness rewarded outer-channel node savings specific to winding, penalized inner-channel savings available to the staggered branch, and required anomalous-density survival on the islands. Second, promoted candidates were rerun as full HFG branch comparisons from uniform, staggered, winding +, and winding − seeds. Only this strict four-branch free-energy comparison is used below as evidence for a ground-state winding result.

IV. MINIMAL C3 SELECTOR

The C3 molecule contains three attractive sites A_0, A_1, A_2 coupled to a central repulsive site C. For the uniform texture the island phase vector is $(1, 1, 1)$. For the two winding textures it is

$$(1, \omega, \omega^2), \qquad (1, \omega^2, \omega), \tag{13}$$

with $\omega = e^{2\pi \mathrm{i}/3}$. The central phase sum obeys

$$1 + \omega + \omega^2 = 0. \tag{14}$$

Thus the winding branches node the active central repulsive site exactly, while the uniform branch drives a central anomalous-density antinode.

The C3 result is best viewed as a mechanism, not as the final physical device. Fixed-number exact-diagonalization diagnostics remain conservative, and full onsite-Hubbard HFB with Hartree and magnetic density relaxation collapses the compact molecule toward nearly normal solutions in the sampled windows. Clusterizing each attractive site does not repair this by itself. Representative cluster recovery scans show that increasing the number of attractive orbitals leaves the strict onsite-Hubbard cluster essentially amplitude-starved. This negative result motivates separating phase selection from condensate formation.

V. C4 OBSTRUCTION AND SPLIT-SCREW REPAIR

For four islands, the relevant phase textures are

$$(1, 1, 1, 1), \qquad (1, \mathrm{i}, -1, -\mathrm{i}),$$
$$(1, -\mathrm{i}, -1, \mathrm{i}), \qquad (1, -1, 1, -1). \tag{15}$$

The first is uniform, the next two are the time-reversed winding partners, and the last is staggered. A single central site is not a unique winding selector, because both winding and staggered textures have zero central phase sum. Moreover, a square molecule usually contains nearest-neighbour in-between normal paths; staggered order cancels those paths exactly. This is the central C4 obstruction.

The successful C4 design rule is to introduce separated diagonal or outer normal paths. In a compact split-centre molecule, this means two distinct normal loci: one coupled to the A_0, A_2 diagonal and one coupled to the A_1, A_3 diagonal. Schematic drawings should therefore treat the structure as screw-separated or effectively lifted out of the plane, not as a single planar crossing site. In the island language, the analogous design is a pair of outside normal paths. They penalize same-phase diagonal pairs

and give winding a saving that staggered order does not share. Constrained compact scans confirm that screw-separated channels, unlike shared outside channels, select winding across broad sampled regions. This remains a phase-selection rule, not yet an unrestricted microscopic superconducting ground-state proof.

VI. MICROSCOPIC BOUNDARY

The compact microscopic models are useful because they remove easy loopholes. They show that winding textures, winding nodes, and degenerate time-reversed partners are not hard to construct. They also show why compact cells are poor final devices. Full density relaxation, finite stiffness, and the uniform or staggered competitors usually erase the winding advantage.

The strongest bulk screw-cell calculation remains a near miss. After releasing the hard winding projection, the best winding branch remains a clean winding texture, with winding weight close to unity, but lies about 5.0×10^{-7} above the uniform branch. A sign-frustrated self-consistency ranking reaches a similar uniform-led margin of about 6.76×10^{-7}. This is evidence for a real metastable winding basin, not an artifact of branch labelling. It is still not a positive bulk ground-state result.

The common failure mode is stiffness and amplitude. Compact models make the loop short and rigid, while a few attractive orbitals do not reliably sustain a robust condensate after Hartree relaxation. This motivates the Josephson-island formulation. The islands or proximity bath supply superconducting amplitude, and the calculation asks whether the normal-channel geometry selects the phase texture.

VII. JOSEPHSON-ISLAND MODEL

The finite island model uses four superconducting islands connected to normal channels. We compare four phase sectors: uniform, staggered, winding +, and winding −. All sectors are iterated to the same self-consistency standard, and the branch free energies are compared after convergence. The design target is a long or soft normal channel that supports a nonwinding antinode and a winding node. The long or soft channel reduces winding stiffness while keeping enough normal-channel anomalous density in the nonwinding branches to create an energy saving.

The promoted positive device is the long-soft outer-channel point labelled `longer-outer2-soft-lower-mu`. It uses

$$U = 2.0, \quad V/U = 0.2, \quad W/V = 1.0, \tag{16}$$

with

$$\mu_{\text{island}} = 0, \quad \mu_{\text{inner}} = -1.0, \quad \mu_{\text{outer}} = -1.6, \tag{17}$$

and geometry parameters

$$\begin{gathered} L = 9, \quad h = 5, \quad h_{\text{inner}} = 3, \\ \text{separation} = 6, \quad \text{outer\_length\_extra} = 2. \end{gathered} \tag{18}$$

The channel hoppings are

$$\begin{gathered} t_{\text{outer channel}} = 0.5, \quad t_{\text{inner contact}} = 0.5, \\ t_{\text{outer contact}} = 1.0. \end{gathered} \tag{19}$$

At this point the strict branch comparison gives

$$F_{\text{wind}} - F_{\text{nonwind}} \simeq -2.386 \times 10^{-3}, \tag{20}$$

with maximum residual 4.996×10^{-5} against a threshold of 5×10^{-5}. A second strict point at $\mu_{\text{outer}} = -1.55$ remains winding-led by approximately -3.019×10^{-3}. Nearby W/V side points are winding-led at moderate convergence but not yet strict, and $\mu_{\text{outer}} = -1.65$ returns to uniform. Thus the current result is a strict existence result and a narrow tuned family, not yet a broad phase pocket.

VIII. DISCUSSION

The result should be stated at the correct level. We have not established a broad robust phase diagram. We have established that a time-reversal-symmetric island Hamiltonian can select a pair of degenerate time-reversed winding minima without external flux. The microscopic studies explain why this requires islands or proximity physics: compact attractive-orbital models either lose amplitude or pay too much winding stiffness. The island model keeps the phase-selection physics while supplying amplitude externally or through larger superconducting reservoirs.

This distinction also clarifies the role of dynamics. Time-dependent HFG and current animations are useful presentation diagnostics because they visualize the selected current-carrying branch. They do not determine the ground state. The ground-state claim rests on the static strict four-branch HFG free-energy comparison.

IX. CONCLUSION

Interference-selected loop supercurrents require two ingredients. First, the normal-channel geometry must make winding suppress anomalous density where nonwinding branches have antinodes. Second, the device must make the winding stiffness small enough for that saving to win. Compact C3 and C4 microscopic models supply the first ingredient and identify the C4 staggered obstruction. Long, soft Josephson-island channels supply the second. The promoted island device therefore provides a controlled existence proof for a spontaneous loop-current state in a time-reversal-symmetric superconducting circuit.

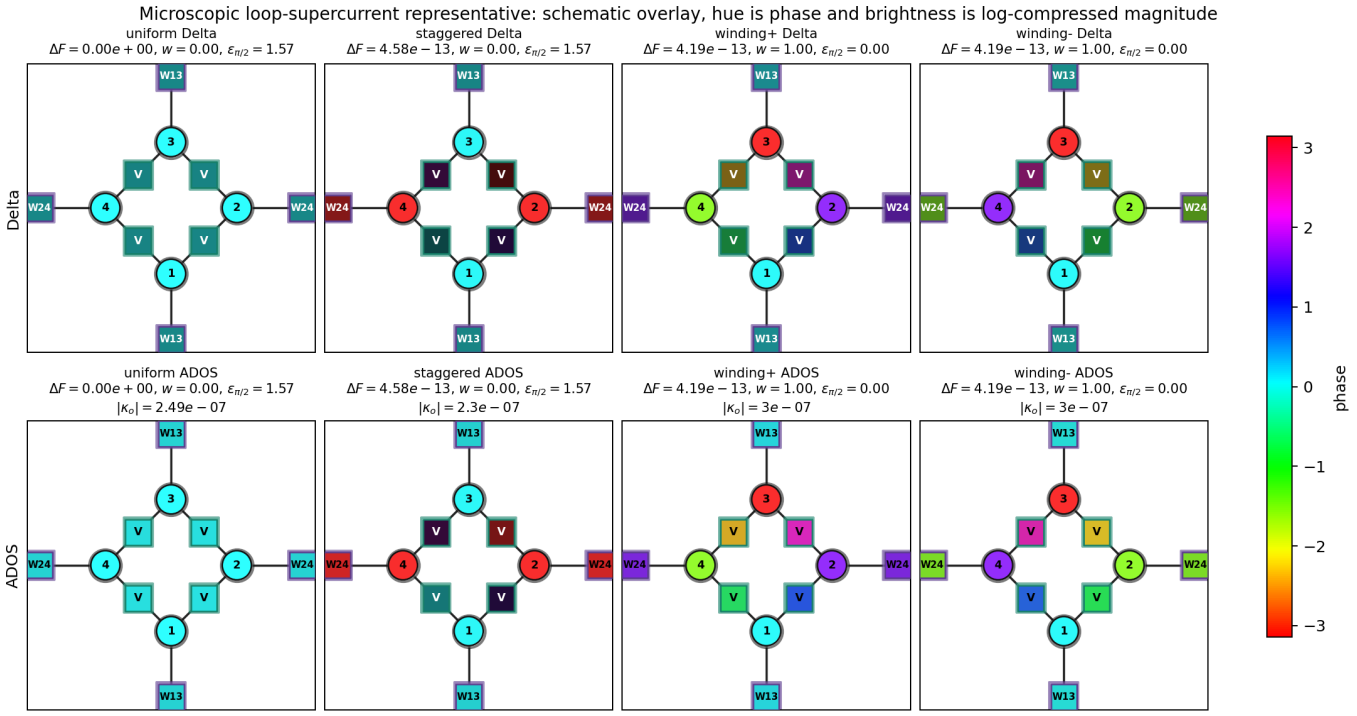

FIG. 3. Compact C4 microscopic anomalous-density examples. Rows show the self-consistent pairing field Δ and anomalous density (ADOS) for uniform, staggered, winding +, and winding − branches in a constrained four-site loop representative. Hue is phase and brightness is log-compressed magnitude. The example illustrates the microscopic texture logic used in the design search: winding branches can retain clean time-reversed phase structure and visible node/antinode rearrangement, even when the compact calculation remains a constrained or near-degenerate diagnostic rather than the final positive island ground-state result.

ACKNOWLEDGMENTS

The calculations and figure provenance are recorded in the QuLab `qulab.research.ljc` module [7].

[1] B. D. Josephson, Physics Letters **1**, 251 (1962).
[2] P. W. Anderson and J. M. Rowell, Physical Review Letters **10**, 230 (1963).
[3] A. J. Leggett, Reviews of Modern Physics **47**, 331 (1975).
[4] M. Sigrist and K. Ueda, Reviews of Modern Physics **63**, 239 (1991).
[5] C. C. Tsuei and J. R. Kirtley, Reviews of Modern Physics **72**, 969 (2000).
[6] L. P. Gor'kov, Soviet Physics JETP **7**, 505 (1958).
[7] H. Sheehy, Qulab loop josephson circuit research module (2026), repository module: qulab.research.ljc.

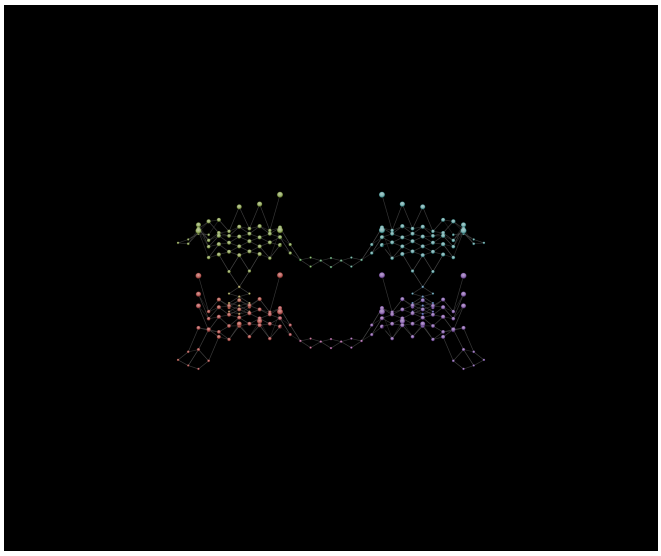

FIG. 4. Three-dimensional rendering of the promoted long-soft island winding branch. Height and colour encode the complex anomalous-density texture on the island and channel sites, making the loop phase twist and outer-channel suppression visible in the same geometry used for the HFG calculation. The Blender and Manim scene files in `qulab.research.ljc.islands` provide the corresponding presentation media; this still is used here only as a geometric visualization.

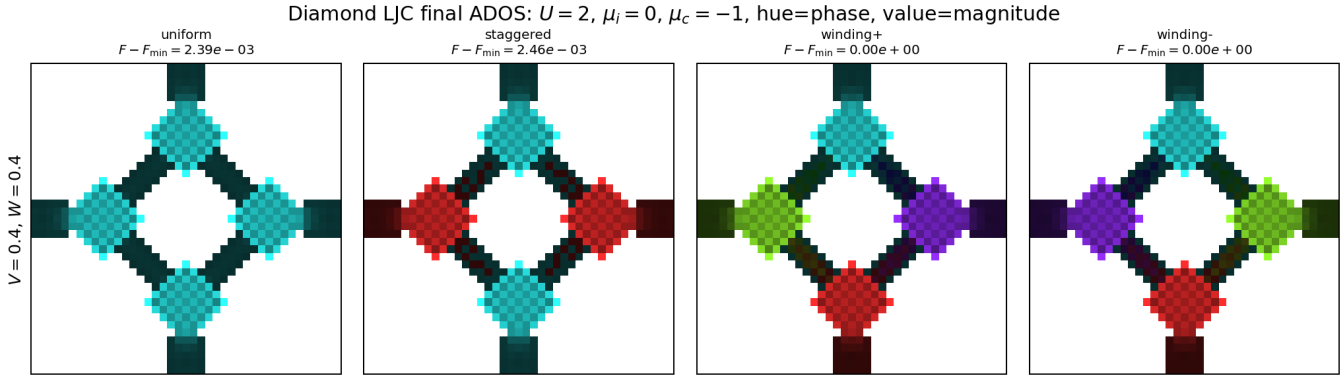

FIG. 5. Complex anomalous-density textures for the promoted island geometry. The four panels show the final self-consistent ADOS for uniform, staggered, winding +, and winding − branches. Hue records complex phase and value records magnitude. The winding branches are time-reversed partners of the same strict minimum.

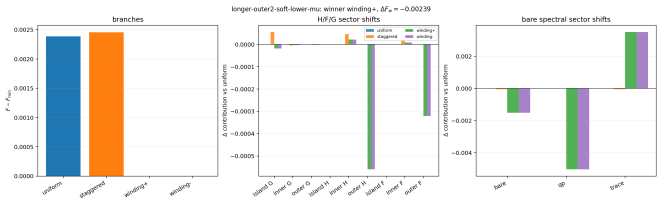

FIG. 6. Free-energy decomposition for the promoted long-soft island point. The branch comparison is the selection evidence: the winding branch is below the best nonwinding branch after the same strict self-consistency criterion is applied to all branches.

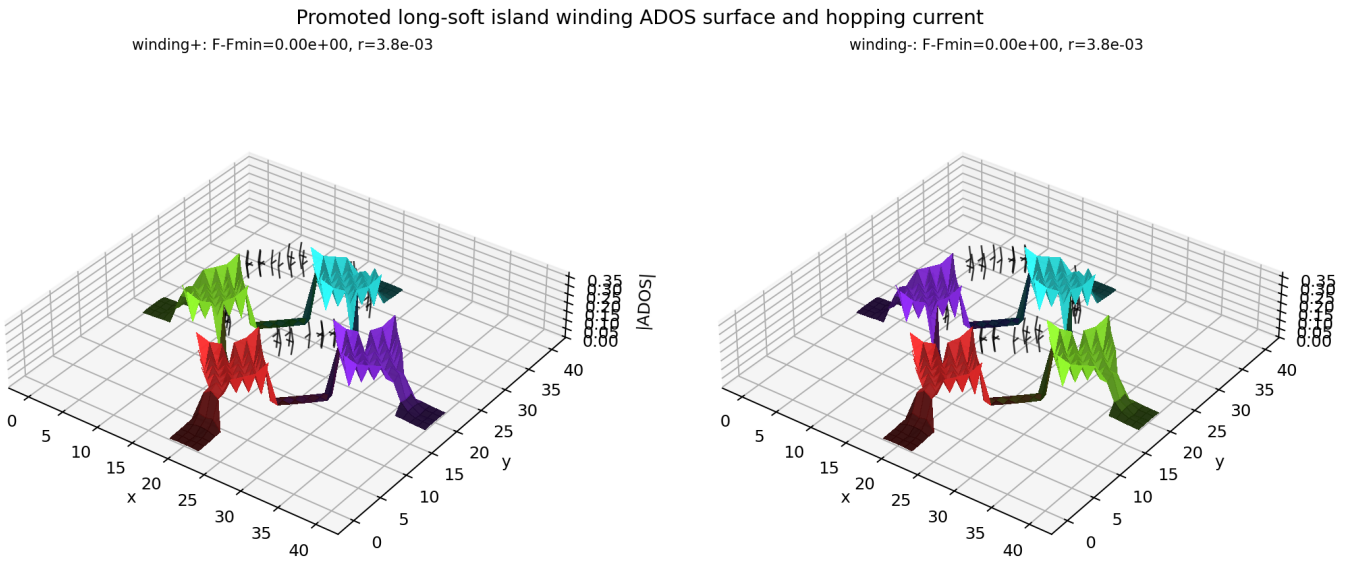

FIG. 7. Current diagnostic for the two promoted winding partners. The two time-reversed branches carry equal-and-opposite circulating hopping-current patterns on top of the self-consistent outer-channel anomalous-density texture. This current plot is an observability diagnostic after free-energy selection, not a replacement for the branch free-energy comparison.